Engineering and Technology Journal e-ISSN: 2456-3358

Volume 09 Issue 07 July-2024, Page No.- 4484-4505

DOI: 10.47191/etj/v9i07.19, I.F. – 8.227

Isothermal and Non-Isothermal Study of 8OCB Liquid Crystal using DSC and Logger Pro.

Grace Petrarca[1], Dipti Sharma (PhD)[2]

[1]Undergraduate student, Emmanuel College Boston, MA, 02115 USA

[2]Supervisor, Emmanuel College, Boston, MA 02115 USA

ABSTRACT: The focus of this research is to explore the isothermal and non-isothermal properties of 4-oxy-4'-cyano-biphenyls (8OCB) Liquid Crystal (LC). This paper reports on the data collected from the technique of DSC and the behavior of 8OCB when heated 0°C/100°C and cooled 100°C/-40°C for ramp rates of 5, 10, and 20 °C/min. The thermal speed, acceleration, and jerk we calculated using the program LoggerPro to further understand the molecules' behavior to observe the effects of repetitive heating and cooling on 8OCB and how that would relate to LC's use in Liquid Crystal Displays (LCDs), specifically looking at if there is any type of degradation in the nematic phase. This data can be used to compare to data collected on the heat flow during, before, and in between the heating and cooling phases to understand how the molecule is further affected by increased ramp rates of constant heating and cooling at times when the temperature is not changing. The isothermal segments of the DSC were seen to have increased heat flow as the ramp rate was increased which is important to consider when applying to the application of nematic LCDs.

KEYWORD: Liquid Crystal (LCs), Phase Change, (Crystalline, Smectic A, Nematic, Isotropic), Liquid Crystal Display (LCD's), 8OCB, LoggerPro, Temperature, Heat Flow, Specific Heat, Isothermal, Non-Isothermal, Ramp Rate, Differential Scanning Calorimetry (DSC)

INTRODUCTION

Matter is classified as anything that has a quantification of mass and takes up a form of volume in space. There are traditionally three states of matter, solid, liquid, and gasses. Solid-state matter can be a crystalline state where the molecules align in a structured orientation that makes it volume-independent of a container. Liquid states contrast to solids as it has an indefinite shape but share the characteristic of a definite volume. Finally, there is a state of gas. There is no definite shape or volume, and atoms can take up their environment with the greatest amount of vibration in random movement. Molecules transition between the states of matter based on increase or decrease in temperature which is the amount of energy the atoms have in freedom of movement [1-3].

There are, however, intermediate states between the three main phases of matter. The intermediate between solid or crystalline states and liquids are molecules called liquid crystals (LCs). LCs exist on the spectrum of crystalline, Smectic C, Smectic A, Nematic, and isotropic. [4]. There are three main types of LCs, thermotropic, lyotropic, and metallotropic. Lyotropic are LCs most affected by temperature and concentration, typically in a solvent of water. Metallotropic are LCs composed of both inorganic and organic material that have a dependency on the concentration of inorganic material. Finally, thermotropic LCs specifically are the type of liquid crystals that are highly manipulated through changes in temperature and the most relevant in technological applications like liquid crystal displays (LCDs) [5-6]. The properties of LCs and how they apply to the application LCDs can be analyzed using DSC.

Differential scanning calorimetry (DSC) is used to study the thermodynamic behavior of diverse types of liquid crystals to determine the phase change and behavior. Many studies are being seen on the phase transitions of liquid crystals. DSC detects the phase change of liquid crystals by measuring heat flow versus temperature within the material. [7-8].

LCD or liquid crystal display is a type of display that uses liquid crystals characteristic of being polymorphic due to different phases exhibiting specific properties. When liquid crystals are placed between layers of glass LCs align either parallel or perpendicular to the applied field when electric current is applied to align and create the projective images. This revolutionary technology became more energy efficient compared to the technology of the time, cathode ray tube monitors [9]. An important phenomenon that allows LCDs to work is the polarization at 90° of each other with liquid crystal sand in the middle that allows polarized light to be twisted and pass through the second polarizer to the pixel and create an image [10-11]. The nCB family has become a significant discovery in LCD research and was discovered by George Grey, first with 5CB LC and there is continuous

research to determine the most effective LC and phase transition for effective and long-lasting LCDs [12].

Nematic LCs is a particular phase in the transition of a liquid crystal from crystalline to isotropic characterized by the order in which the molecules are oriented in the nematic state [13]. Specifically relating to liquid crystals and technology, liquid crystals, make up liquid crystal displays utilizing the nematic phase as the crystals in nematic, can align themselves with axes in parallel, and can be applied to an electric field that can change the orientation of the molecules in the layer of liquid, manipulating the optical properties [14]. This research aims to explore the nOCB family by looking at the properties of 8OCB.

8OCB has a biphenyl structure with octyloxy and cyano groups at 4,4'-positions (4-oxy-4'-cyano-biphenyls). [15]. The molecular formula is $C_{21}H_{25}ON$. This differs from the nCB family as there is the addition of oxygen in the CB tail. Both 8OCB and 8CB have the transition of crystalline to smectic A, nematic and finally isotropic. However, the addition of oxygen increases the dipole moment and therefore stabilizes the phases of the LC to higher temperatures relative to 8CB, the addition of oxygen being a contributing factor as it increases the weight and stability of the molecule. [16-18]. The characteristics of 8OCB can be translated into quantitative representation through the program LoggerPro to further understand its potential.

LoggerPro by Vernier is a data collection software that can connect to laboratory equipment in order to collect, analyze and interpret data from various sensory equipment [19]. From the state of collection, LoggerPro is able to devise, graphical, representations, propagate statistics and create models that represent the experiment results as a college student Logger Pro has been instrumental and being able to understand how real-world data is collected in interpreted to solve the problems at hand research aims to solve [20].

Our interests in 8OCB in this research are exploring the thermodynamic properties of its structure that allow for 8OCB to have distinct properties in its various phases. Understanding the behavior of 8OCB, we can interpret how its properties as a Liquid Crystal can be manipulated in technologies like liquid crystal displays (LCDs). As LCDs utilize the nematic phase of liquid crystals, it is important to understand how the LCs are affected by heat as LCDs take advantage of their thermotropic nature to best align the crystals between polarizable sheets that are parallel to each other to twist light transition through the field to create images on LCDs. However, constant heating and cooling of the crystals during technology usage affects properties of the crystal that can be measured using differential scanning calorimetry (DSC), which enables the ability to understand how heatf low, rate of temperature manipulation and time affect the molecule's overall. Interpreting this data in the program LoggerPro allows us to visualize the molecules during different stages of heating and cooling inorder to explore the possibilities of nCB or nOCB LCs and their possibilities in the application of LCDs.

EXPERIMENTAL SECTION

The Octyl Oxy Cyanobiphenyl (8OCB) is a thermotropic liquid crystal from nOCB family. It has an Oxygen atom in the molecule. The molecular weight of 8OCB is 307.43 g/mol. For this study, a small amount 5.0 mg of 8OCB is taken in an aluminum cup and then sealed with its lid on top of it. This cup and lid is the part of the instrument that is used to study the thermal behavior of 8OCB. The instrument used for this study is called Differential Scanning Calorimetry (DSC). The sealed cup and lid with 8OCB sample is then taken into DSC, model DSC 214 instrument from the NETZSCH company at WPI, chemistry and biochemistry department, Worcester, MA. This sample of 8OCB is heated from -40 °C to 100 °C and then cooled back from 100 °C to -40 °C with three different 5 °C/min, 10 °C/min, and 20 °C/min heating and cooling ramp rates. The data collected from DSC instrument is used for further study. The data showed how heat flows in the sample with time and temperature. These data is taken to Logger Pro for further detailed analysis of 8OCB thermal behavior. The thermal behavior of 8OCB is done in two ways, a) non-isothermally - when the temperature of the sample is set to one constant temperature and heat flow of the sample is measured as a function of time, b) Isothermally - when the temperature of the sample is changed, and corresponding heat flow is measured.

The molecular structure of 8OCB molecule consists of two benzene rings, one cyano group, one oxygen between benzene and C-H groups, and eight C-H groups in the tail. The 2D and 3D molecular structure of 8OCB can be seen in **Figure 1 and Figure 2.**

Figure 3 documents phase transitions of liquid crystal molecules, similar to the 8OCB in this study. The crystalline state is characteristic of the LC molecules being organized in ordered rows and columns. With the increasing introduction of heat, smectic C arises as the molecules retain their order rows and columns with a uniform angular tilt from the normal. Following is smectic A, which shares organization retained in the columns, but not the rows as neighboring molecules begin to interact. Again, as more heat is introduced, the nematic phase characteristically loses uniformity in both the rows and columns, mirroring liquid properties, but retaining uniform direction. Finally, the weakest of the transition phases, isotropic, has no quality of order in rows, columns or orientation.

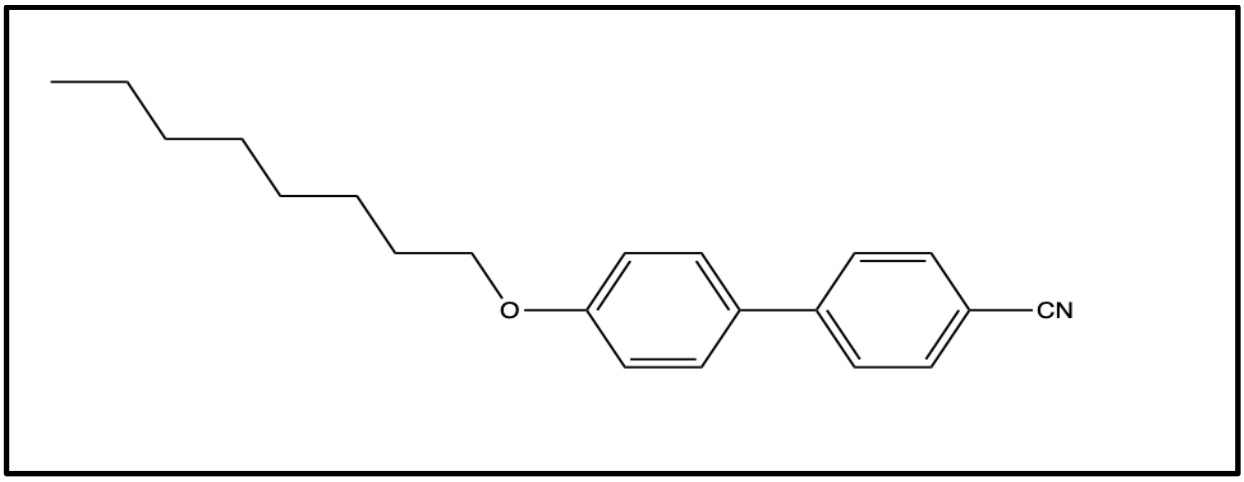

Figure 1. 2D image of 8OCB Liquid Crystal Molecule.

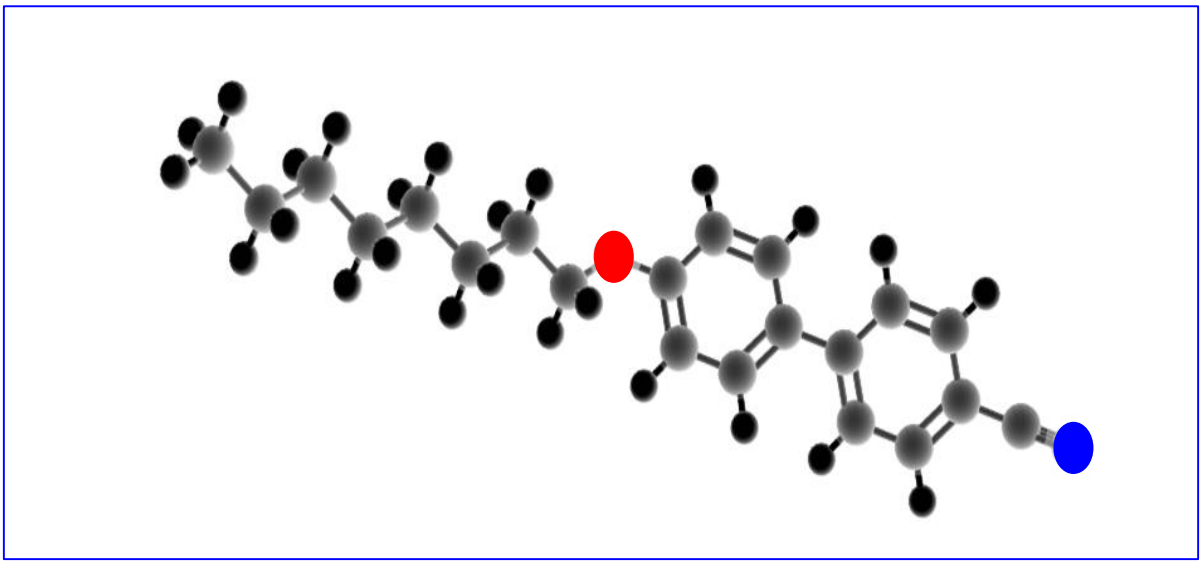

Figure 2. 3 D image of 8OCB Liquid Crystal Molecule.

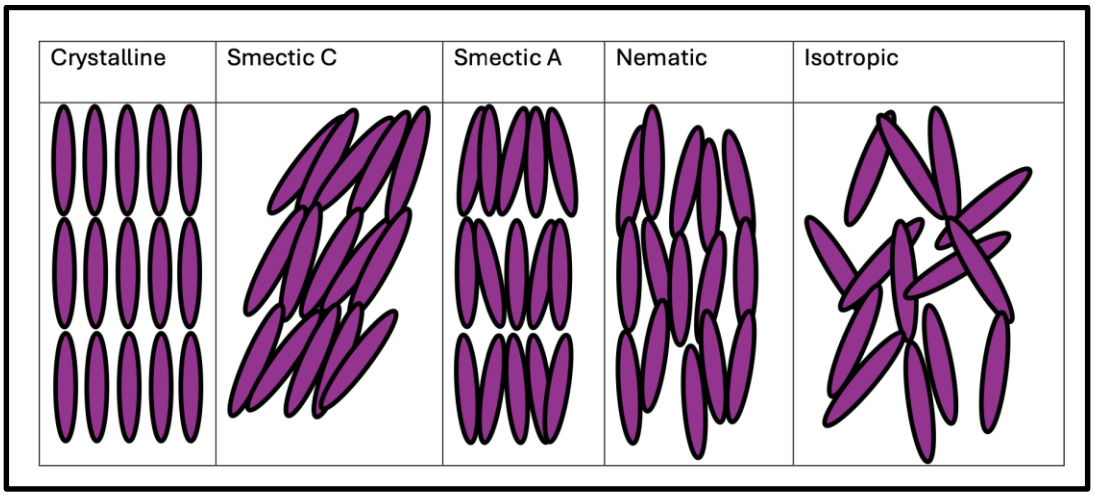

Figure 3. Molecular arrangement of liquid crystals in crystalline (C), Smectic C (SmC), Smectic A (SmA), Nematic (N), and Isotropic (I).

THEORETICAL BASIS

The basic theory involved in this study is thermodynamics of 8OCB. The 8OCB molecules follow changes with temperature and time when heat is passed into it. So, our goal is to see how heat flow can be changed by the state of 8OCB molecules when heat is passed into it with time and temperature. We studied the behavior of 8OCB in two ways, a) Non-Iso Thermally when temperature is changed and b)

Isothermally when temperature is not changed but time is changed. I

According to thermodynamics, the heat (Q) can be related to mass (m), specific heat capacity of the sample (Cp) and change is in temperature ($\boldsymbol{\Delta T}$) as shown in equation 1. Since DSC measures heat flow instead of just heat, then the heat flow (dQ/dt) can be shown as a function of heating rate (dT/dt) in equation 2.

$$\boldsymbol{Q = m * Cp * \Delta T} \quad -1$$

$$\boldsymbol{\frac{dQ}{dT} = m * Cp * \frac{dT}{dt}} \quad -2$$

For Non-Isothermal Study, temperature needs to be changed and heat flow should be recorded. The heat flow can be normalized by mass so that the amount of mass of the sample should not bring any effect on it. Hence the equation 2 can be modified then to equation 3. The heat flow (HF) can also be written as shown in equation 4.

$$\frac{dQ}{dT}/m = Cp * \frac{dT}{dt} \quad -3$$

$$\text{HF} = \frac{dQ}{dT}/m = Cp * \frac{dT}{dt} \quad -4$$

Now, we will take derivatives of HF. The first derivative of the HF gives the thermal speed (v) shown in Equation 4, that gives the change in heat flow with a given time ($\frac{d(HF)}{dt}$).

$$v = \frac{d(HF)}{dt} = Cp * \frac{d^2(Q)}{dt^2} \quad -5$$

The second derivative of the heat flow equation gives the Thermal acceleration (a) shown in equation 6.

$$a = \frac{d(v)}{dt} = \frac{d^2(HF)}{dt^2} = Cp * \frac{d^3(Q)}{dt^3} \quad -6$$

$$J = \frac{d(a)}{dt} = \frac{d^3(HF)}{dt^2} = C * \frac{d^4(Q)}{dt^4} \quad -7$$

Similarly, the third derivative of the heat flow equation gives the thermal jerk (J), shown in equation 7.

For Isothermal study of 8OCB, the temperature is set to one constant temperature and time is changed while heat flow is measured by DSC.

Detailed results of 8OCB can be seen in the result section.

RESULTS

The isothermal and non-isothermal study of 8OCB Liquid Crystal was analyzed using the technique of DSC by subjecting the sample to three different runs of heating and cooling (5, 10 and 20 °C/min). The three different runs were broken down into 13 segments and the breakdown of the behavior of each segment can be found in Table 1. The individual temperatures of the crystalline (T_k), smectic (T_sm), and nematic (T_n) peaks can be found in Table 2 for each of the segments of heating and cooling for all three runs. The graphical representation of data in Table 2 can be found in **Figures 5, 10, 15, 20, 25 and 30**. These peaks represent at what temperature the phase change occurred.

Furthermore, the heat flow and time for the heating and cooling segments can be found in Table 3-5, accounting for where in the 100 minute DSC run the the crystalline, smectic and nematic transition occurred and how thermal speed 9 (blue), acceleration (green) and jerk (orange) relate to their behavior of being cooled and reheated, these graphical models can be found in the highlighted colors above for each segment. The thermal speed/velocity is a measurement of the speed of particles in motion relating to their state of matter and indirectly relating to the temperature of the particle. Thermal acceleration is a measure of the speed of thermal heat exchange a particle is experiencing over time. Thermal jerk measures how fast the thermal acceleration is changing with respect to time, quantifying how gradual or "smooth" the transition in heat flow in particles is. See **Figure 37** for the graphical depiction of the entire DSC data set with all 13 segments together.

Table 1. Break down of segments during DSC runs of 5 (seg. 1-4), 10 (seg. 5-8) and 20 (seg. 9-12) °C/min. The table below represents the 13 segment run of the DSC on 8OCB for 3 different ram rat runs of 5, 10 and 20 (K/min). These segments will be referred to as to locate where in the DSC run data is being referred to. The even segments (2, 4, 6, etc) refer to non-isothermal movements of heat or cooling while the odd segments (1, 3, 5, etc) are isothermal occurrences. The non-isothermal segment data extrapolates from Table 2-5 and **Figures 4- 33**. Isothermal data can be found in **Figure 34.**

#SEGMENT:	S1-13/13
#SEG. 1:	0°C/00:01/0°C
#SEG. 2:	0°C/5.0(K/min)/100°C
#SEG. 3:	100°C/00:01/100°C
#SEG. 4:	100°C/5.0(K/min)/-40°C
#SEG. 5:	-40°C/00:01/-40°C
#SEG. 6:	-40°C/10.0(K/min)/100°C
#SEG. 7:	100°C/00:01/100°C

#SEG. 8:	100°C/10.0(K/min)/-40°C
#SEG. 9:	-40°C/00:01/-40°C
#SEG. 10:	-40°C/20.0(K/min)/100°C
#SEG. 11:	100°C/00:01/100°C
#SEG. 12:	100°C/20.0(K/min)/-40°C
#SEG. 13:	-40°C/00:02/-40°C

Table 2: Peak temperature of 8OCB for three different runs.

Rate °C/min	**Cycle**	**Tk (°C) of peak**	**Tsm(°C) of peak**	**Tn (°C) of peak**
5	**Heat (seg. 2)**	**59.78**	**70.50**	**83.20**
	Cool (seg. 4)	**27.12**	**47.35**	**82.12**
10	**Heat (seg. 6)**	**59.80**	**70.44**	**83.70**
	Cool (seg. 8)	**24.61**	**47.60**	**81.99**
20	**Heat (seg. 10)**	**60.84**	**70.80**	**84.21**
	Cool (seg. 12)	**21.71**	**49.88**	**81.00**

Table 3: Peak Values for time and thermal quantities of 8OCB for heating and cooling at rate 5°C/min.

Derivative	t_k1 (min)	Hf_k1 (mW/ mg)	t_k2 (min)	Hf_k2 (mW/ mg)	t_sm (min)	Hf_ksm (mW/ mg)	t_n1(min)	Hf_n1 (mW/ mg)	t_n2 (min)	Hf_n2 (mW/ mg)
Seg 2										
speed	12.62	10.36	13.10	-11.62	14.93	0.22	17.60	3.62	17.73	-1.71
Acceleration	12.60	70.90	13.02	-178.0	13.27	67.2	17.59	123.0	17.63	-79.10
Jerk	12.54	955	12.93	-4033	13.03	4234	17.59	4748	17.60	-7923
Seg 4										
Speed	25.58	-3.96	25.69	0.95	28.20	-0.11	36.22	-11.45	36.71	18.99
Acceleration	25.57	-160	25.64	74	26.78	-6.0	36.12	-144.0	36.67	406.0
Jerk	25.59	-6373	25.63	8984	-	-	36.75	-13628	36.75	7289

Table 4: Peak Values for time and thermal quantities of 8OCB for heating and cooling at rate 10°C/min.

Derivative	t_k1 (min)	Hf_k1 (mW/ mg)	t_k2 (min)	Hf_k2 (mW/ mg)	t_sm (min)	Hf_ksm (mW/ mg)	t_n1(min)	Hf_n1 (mW/ mg)	t_n2 (min)	Hf_n2 (mW/ mg)
Seg 6										
Speed	60.84	12.20	61.08	-20.22	62.00	0.33	63.33	5.32	63.38	-2.21
Acceleration	60.79	55	61.04	-294	62.02	16	63.31	311	63.36	-154
Jerk	60.91	2390	61.06	-8086	61.07	15250	63.28	22537	63.33	-33596
Seg 8										
Speed	67.86	-6.0	67.93	1.4	69.14	-0.6	73.50	-32.2	73.66	28.6
Acceleration	67.83	-416	67.86	134	-	-	73.37	-510	73.55	782
Jerk	67.80	-32187	67.81	36949	-	-	73.35	-11446	73.40	37448

Table 5: Peak Values for time and thermal quantities of 8OCB for heating and cooling at rate 20°C/min.

Derivative	t_k1 (min)	Hf_k1 (mW/ mg)	t_k2 (min)	Hf_k2 (mW/ mg)	t_sm (min)	Hf_ksm (mW/ mg)	t_n1(min)	Hf_n1 (mW/ mg)	t_n2 (min)	Hf_n2 (mW/ mg)
Seg 10										
Speed	85.95	24.9	86.14	-31.0	86.40	0.1	87.18	7.6	87.24	-2.5
Acceleration	85.92	165	86.11	-636	86.50	49	87.18	632	87.22	-294
Jerk	-	-	86.10	-21634	-	-	87.15	78833	87.19	-97162
Seg 12										
Speed	89.95	-8.5	90.44	1.9	91.51	2.2	92.89	-32.2	93.07	26.6
Acceleration	89.95	-934	90.00	262	91.49	339	92.75	-330	93.05	876
Jerk	89.95	-135853	89.97	118583	91.50	51106	92.91	-27945	93.04	43519

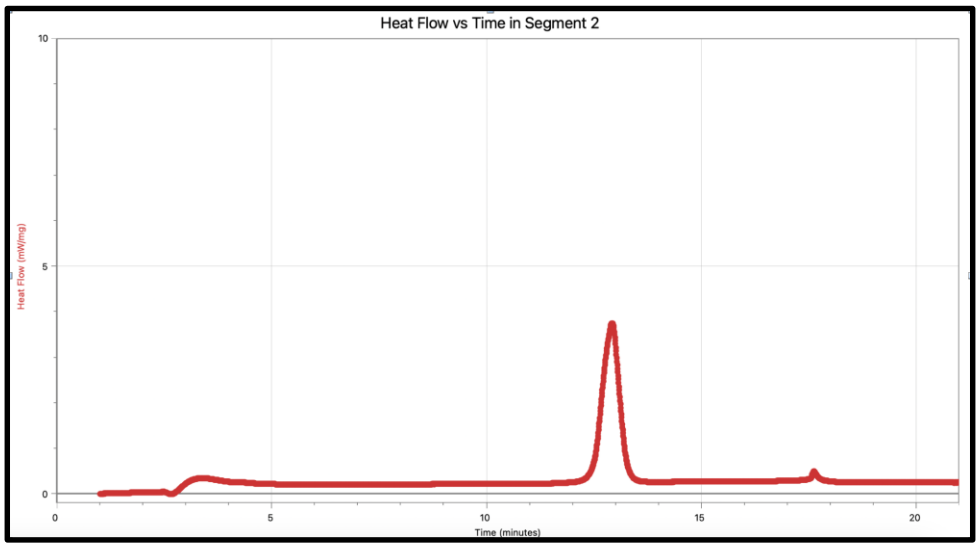

Figure 4. Heat Flow vs.Time graph for 8OCB for heating at rate 5°C/min.

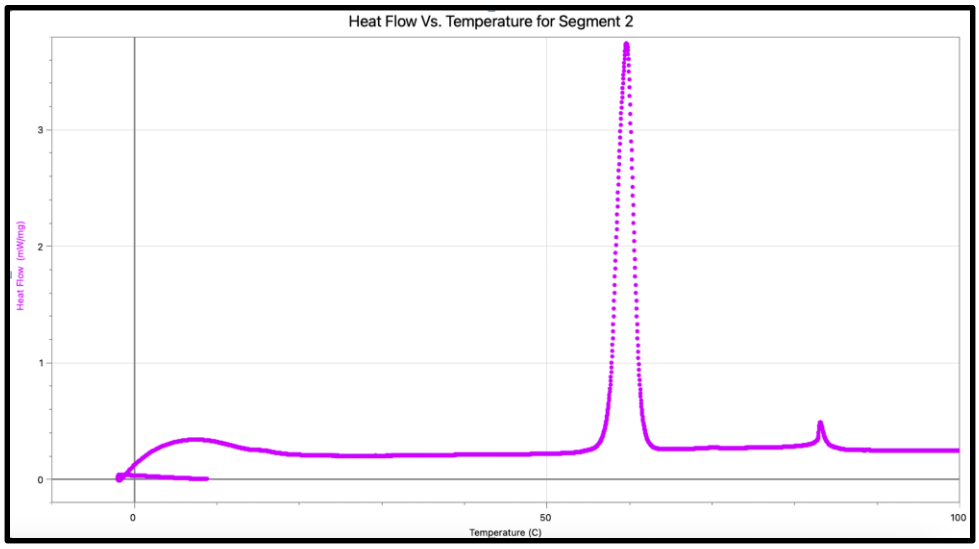

Figure 5. Heat Flow vs.Temperature graph for 8OCB for heating at rate 5°C/min.

.

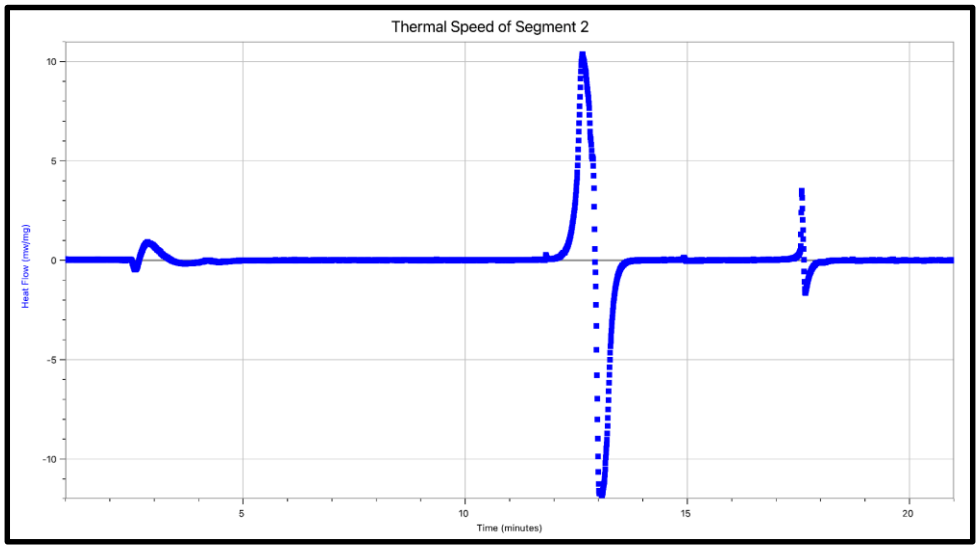

Figure 6. Thermal speed vs time graph for 8OCB for heating at rate 5°C/min.

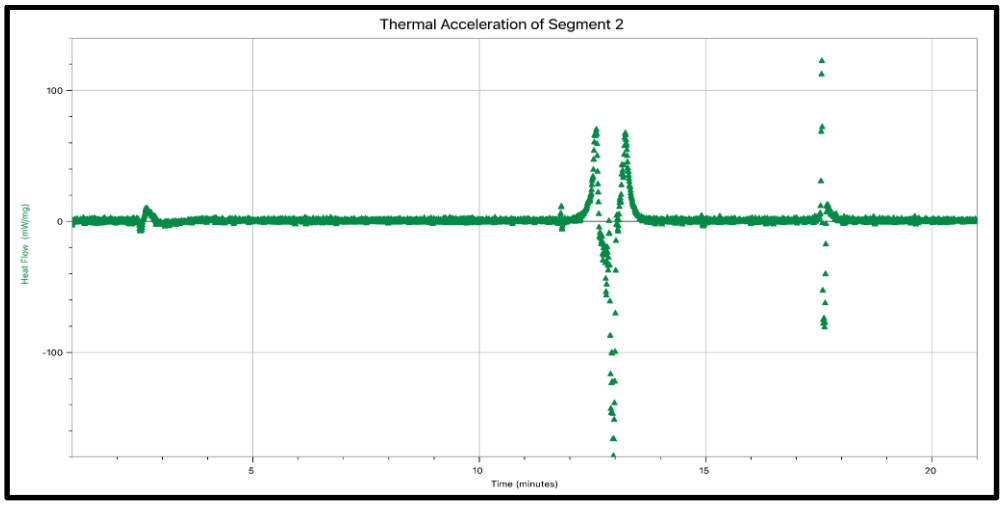

Figure 7. Thermal acceleration vs. Time graph for 8OCB for heating at rate 5°C/min.

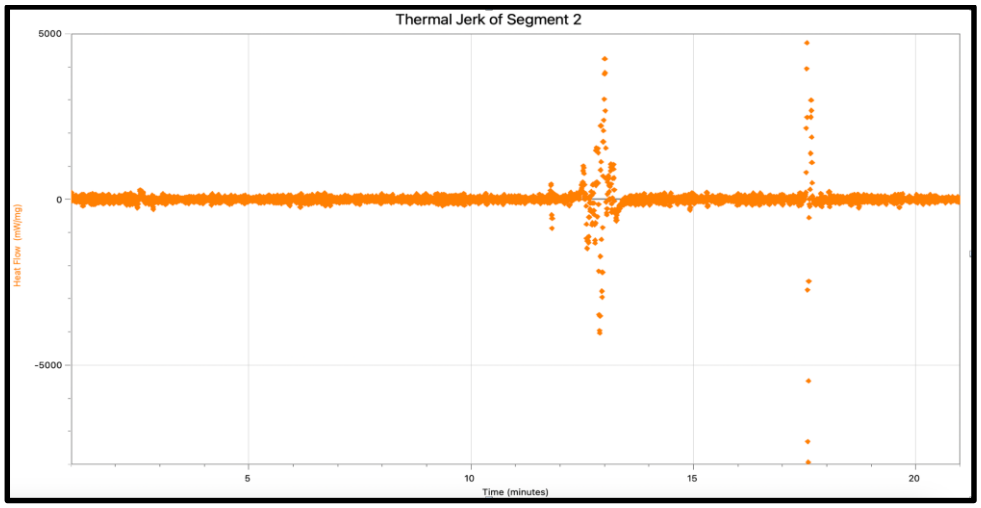

Figure 8. Thermal Jerk vs. Time graph for 8OCB for heating at rate 5°C/min.

Figures 4-8 represent the data collected for segment 2 (0°C/5.0(K/min)/100°C). Figure 4 shows the heat flow and time for the heating of 8OCB LC with peaks for crystalline (k), smectic (sm) and nematic (n). **Figure 5** compares the temperature and heat flow of the phase peak whose data can be found in Table 2. **Figures 6-8** are comparisons of the heat flow and time using the quantitative representations of thermal speed, acceleration and jerk, equations 5-7 were used to create the derived graphical representations using LoggerPro. The peak values for the derivative graphs are reported in Table 3.

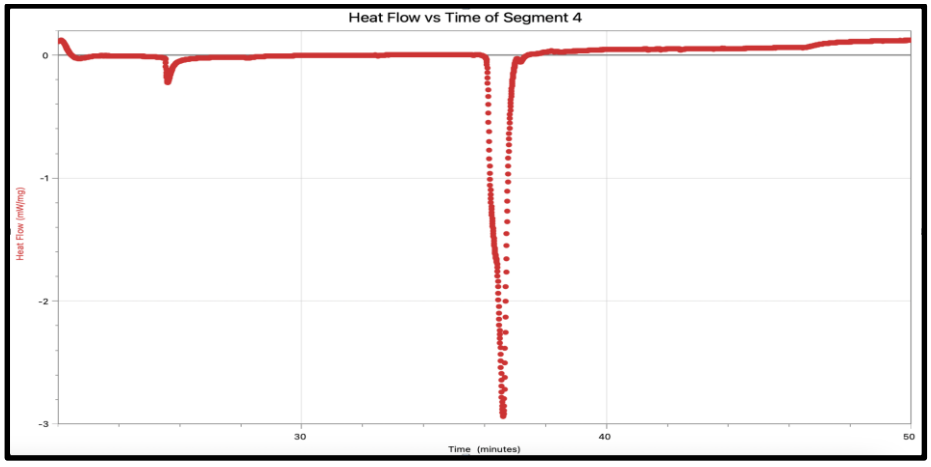

Figure 9. Heat Flow vs.Time graph for 8OCB for cooling at rate 5°C/min.

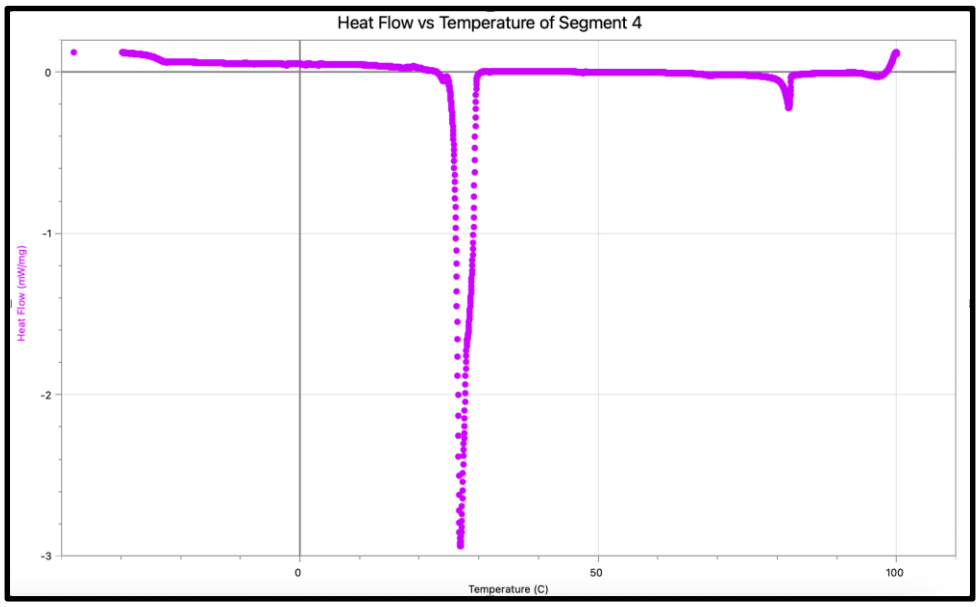

Figure 10. Heat flow vs. Temperature graph for 8OCB for cooling at rate 5°C/min.

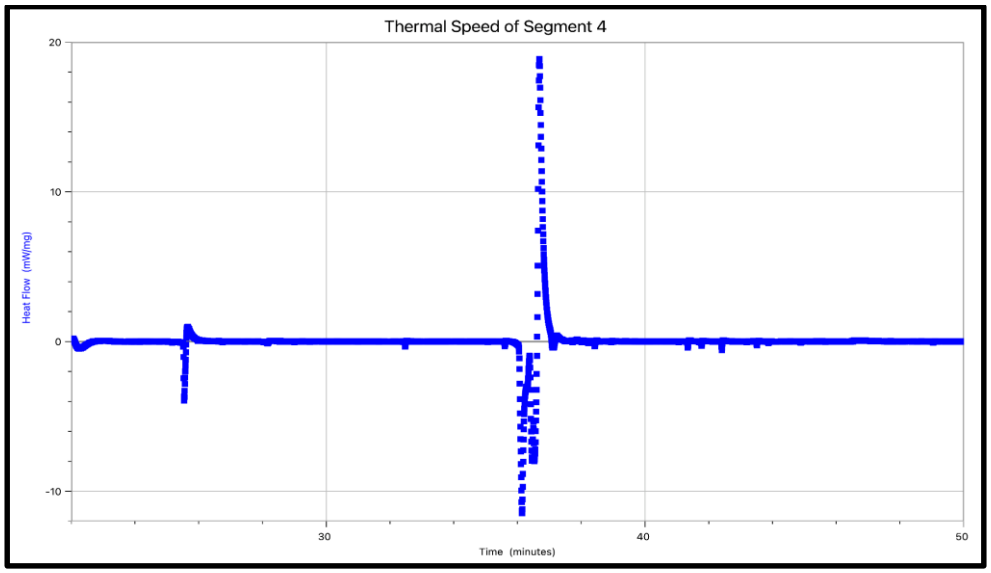

Figure 11. Thermal speed vs time graph for 8OCB for cooling at rate 5°C/min.

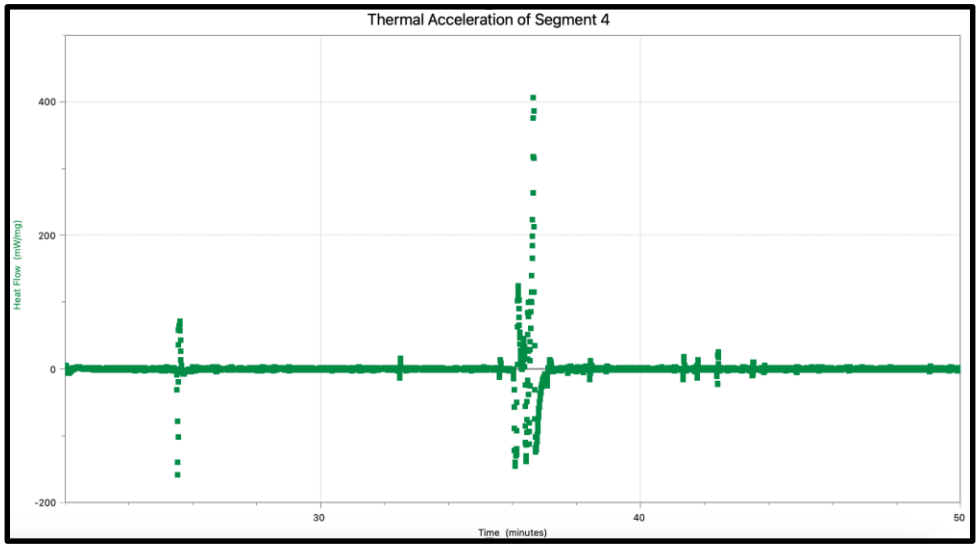

Figure 12. Thermal acceleration vs. Time graph for 8OCB for cooling at rate 5°C/min.

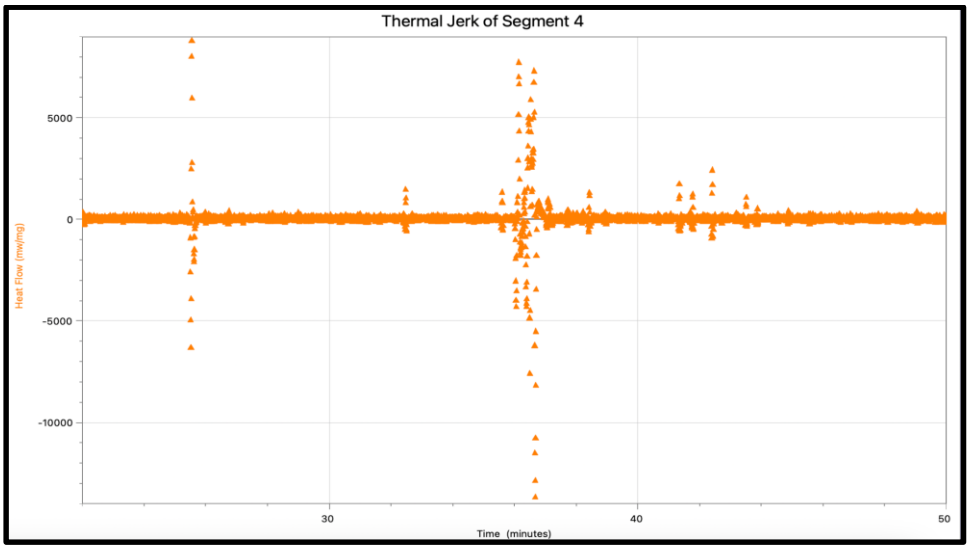

Figure 13. Thermal Jerk vs. Time graph for 8OCB for cooling at rate 5°C/min.

Figures 9-13 represent the data collected for segment 2 (0°C/10.0(K/min)/100°C). **Figure 9** shows the heat flow and time for the cooling of 8OCB LC with peaks for crystalline (k), smectic (sm) and nematic (n). **Figure 10** compares the temperature and heat flow of the phase peak whose data can be found in Table 2. **Figures 6-8** are comparisons of the heat flow and time using the quantitative representations of thermal speed, acceleration, and jerk, equations 11-13 were used to create the derived graphical representations using LoggerPro. The peak values for the derivative graphs are reported in Table 3.

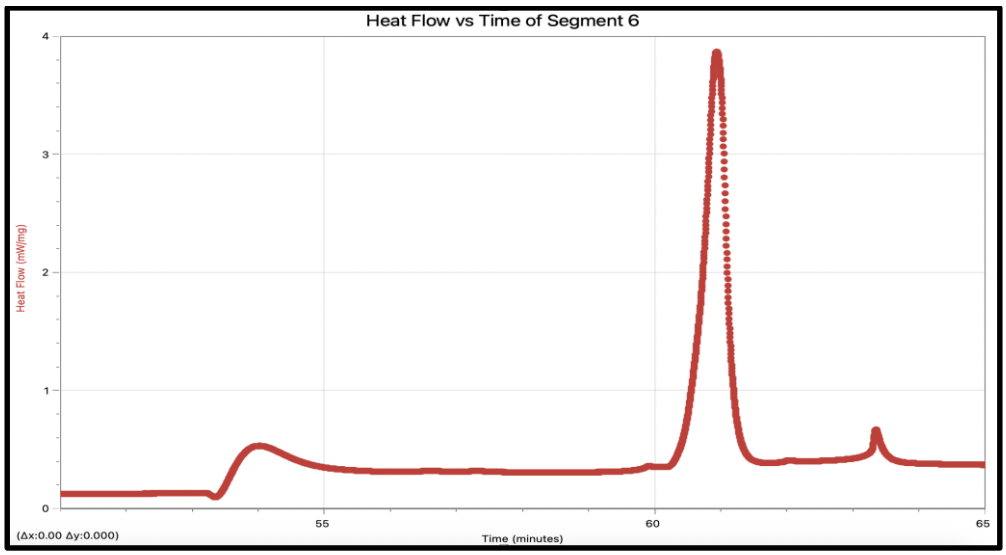

Figure 14. Heat Flow vs.Time graph for 8OCB for heating at rate 10°C/min.

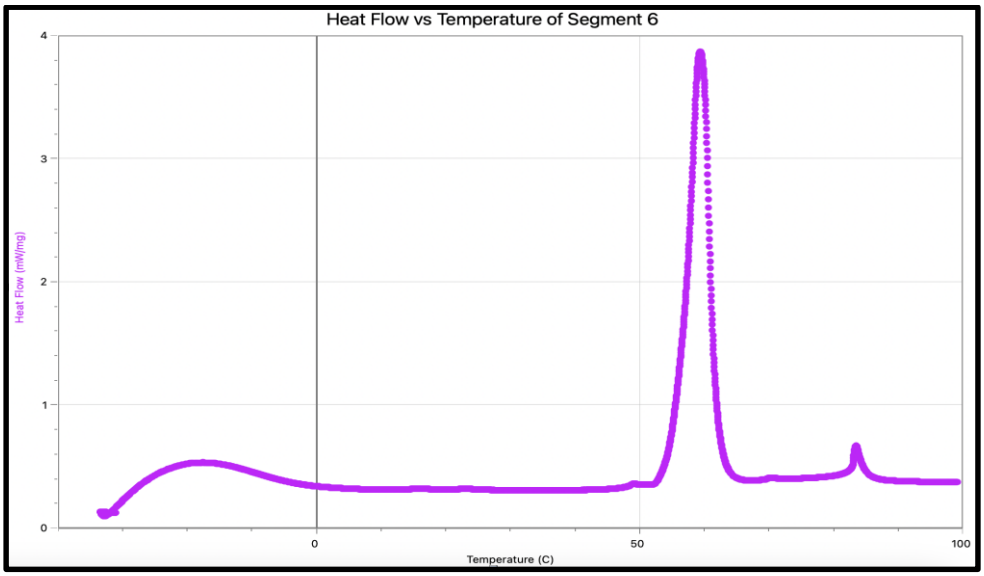

Figure 15. Heat Flow vs.Temperature graph for 8OCB for heating at rate 10°C/min.

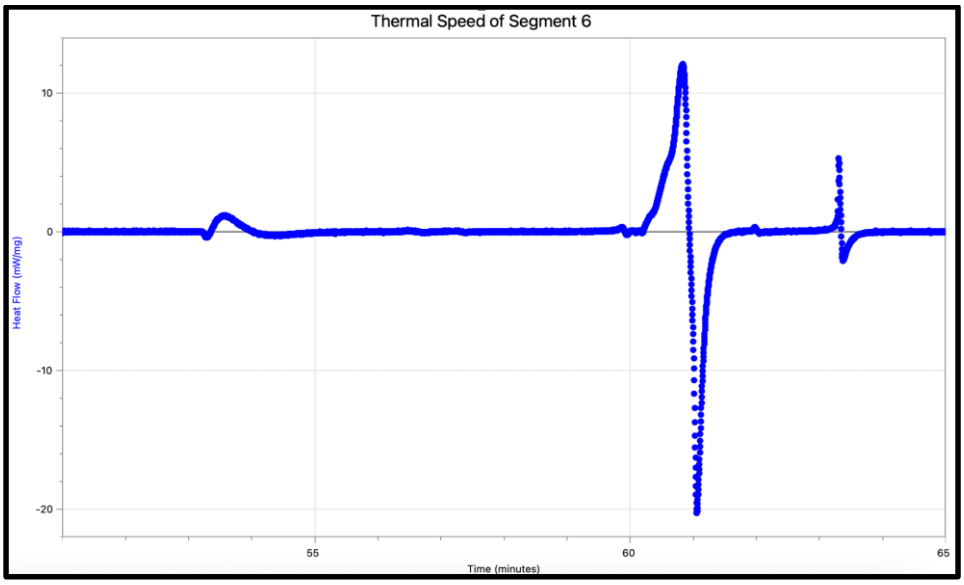

Figure 16. Thermal speed vs time graph for 8OCB for heating at rate 10°C/min.

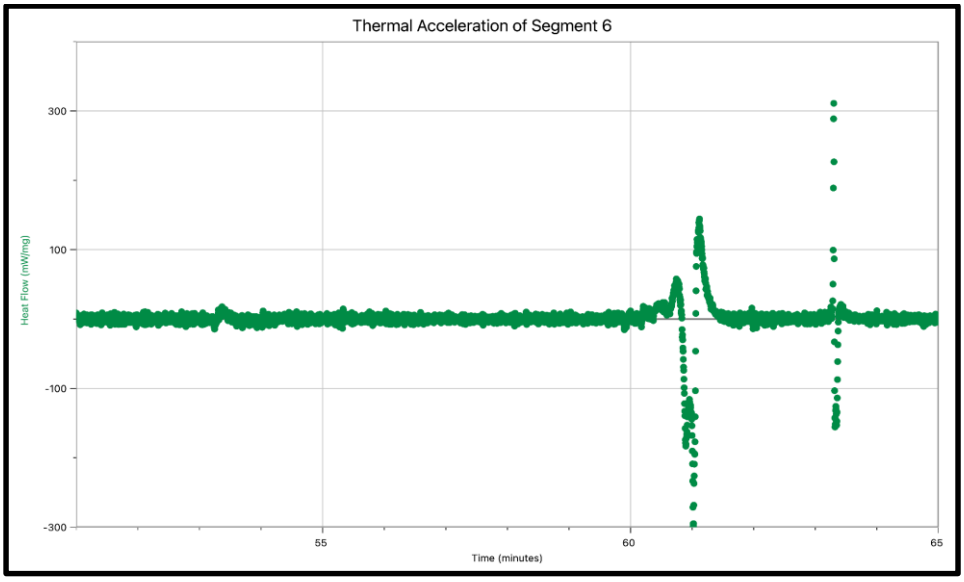

Figure 17. Thermal acceleration vs. Time graph for 8OCB for heating at rate 10°C/min.

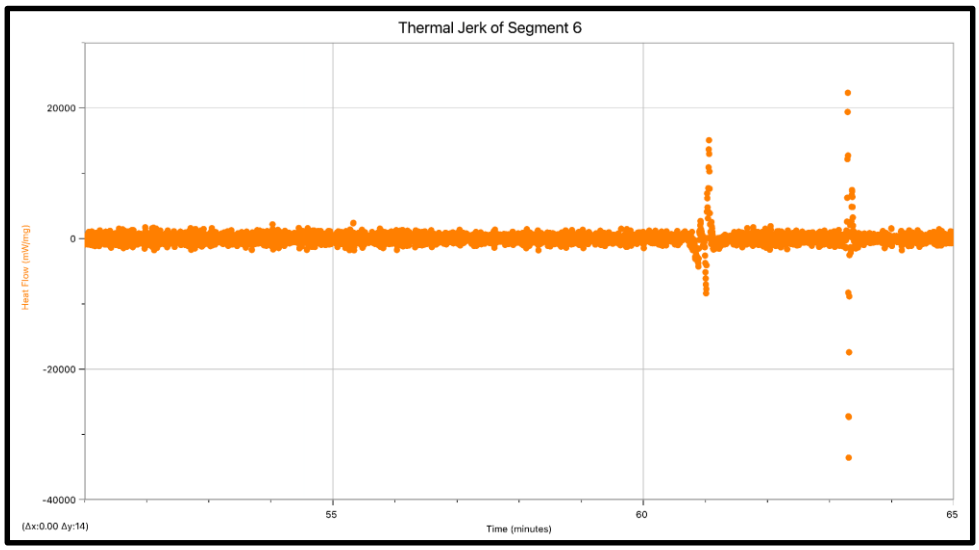

Figure 18. Thermal Jerk vs. Time graph for 8OCB for heating at rate 10°C/min.

Figures 14-18 represent the data collected for segment 2 (0°C/10.0(K/min)/100°C). **Figure 14** shows the heat flow and time for the heating of 8OCB LC with peaks for crystalline (k), smectic (sm), and nematic (n). **Figure 15** compares the temperature and heat flow of the phase peak whose data can be found in Table 2. **Figures 16-18** are comparisons of the heat flow and time using the quantitative representations of thermal speed, acceleration, and jerk, equations 11-13 were used to create the derived graphical representations using LoggerPro. The peak values for the derivative graphs are reported in Table 4. Due to the increased heat flow, the time to take for 8OCB peak from k_1 to n_2 was 2.54 minutes versus the first run of 5.0(K/min) which took place over 5 minutes. There is also a noticeable difference in the heat flow of the derivative graphs for the thermal speed, acceleration and jerk. Though fromTable 2 the sample reached about the same temperature for its peak transition phases, the motion of the particles and their heat flow is greatly increased.

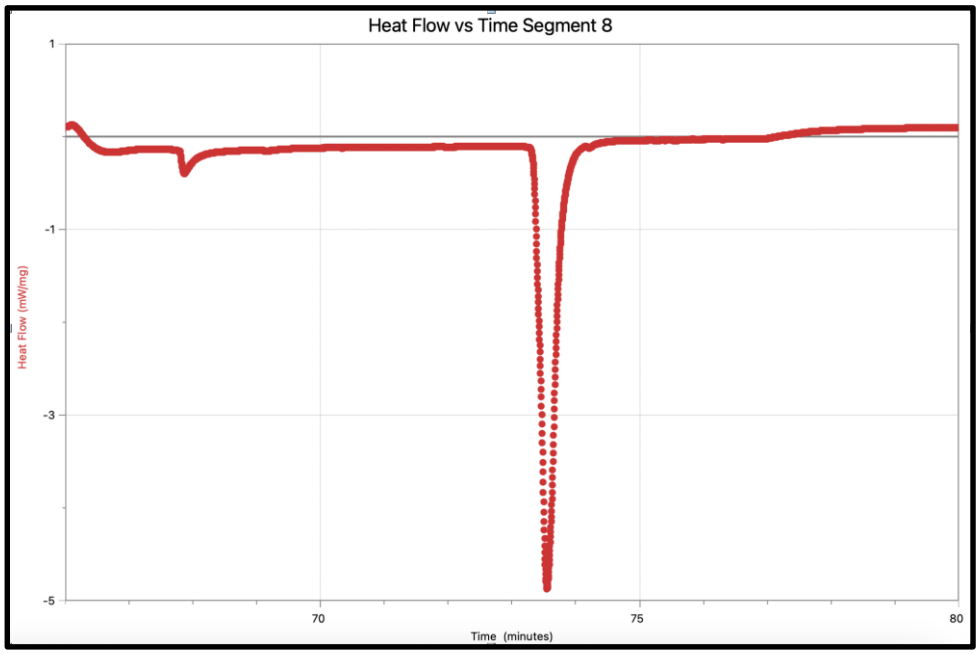

Figure 19. Heat flow vs. Time graph for 8OCB for cooling at rate 10°C/min.

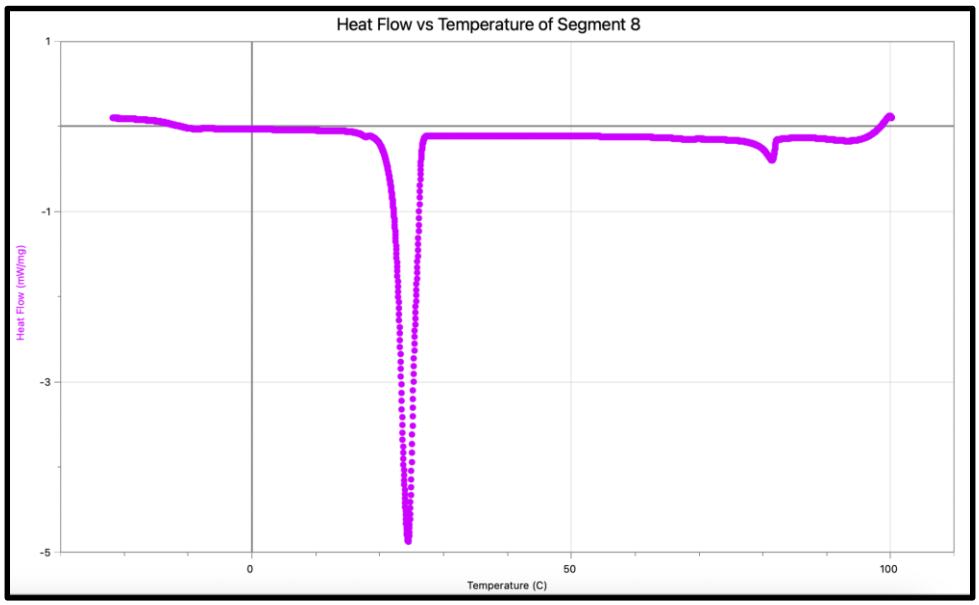

Figure 20. Heat flow vs. Temperature graph for 8OCB for cooling at rate 10°C/min.

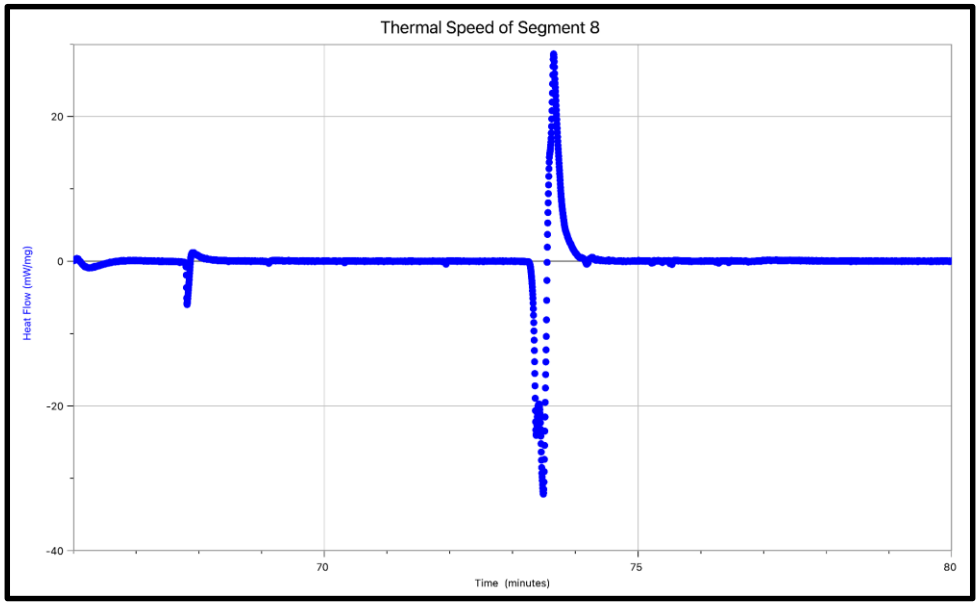

Figure 21. Thermal speed vs time graph for 8OCB for cooling at rate 10°C/min.

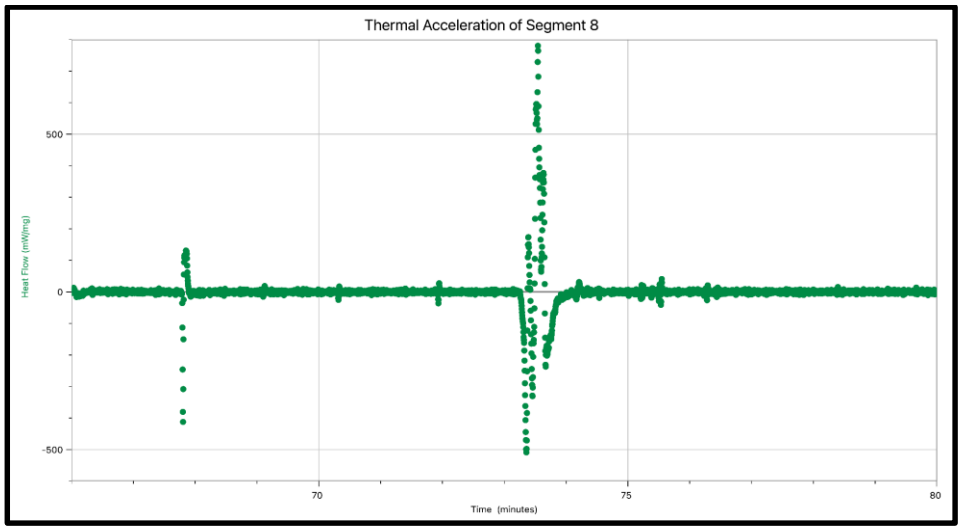

Figure 22. Thermal acceleration vs. Time graph for 8OCB for cooling at rate 10°C/min.

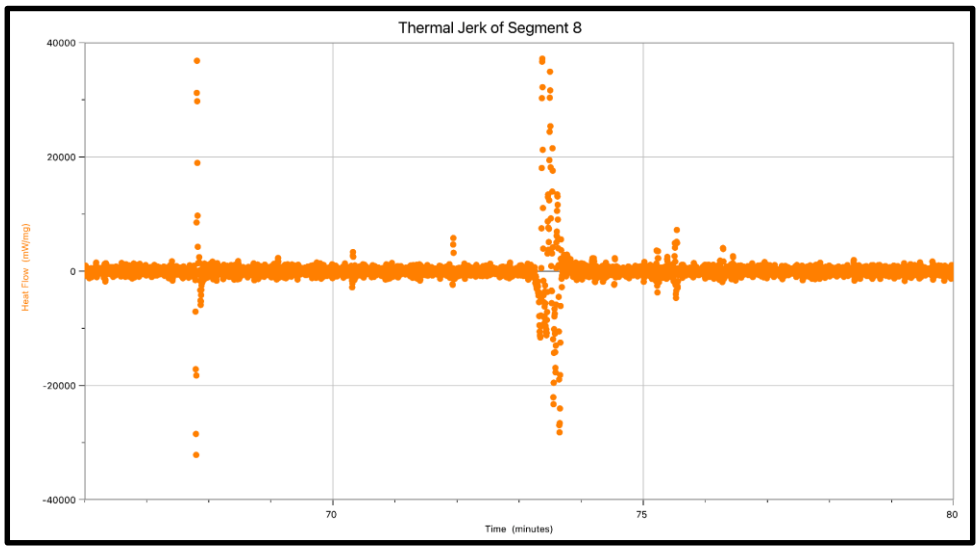

Figure 23. Thermal Jerk vs. Time graph for 8OCB for cooling at rate 10°C/min.

Figures 19-23 represent the data collected for segment 2 (0°C/10.0(K/min)/100°C). **Figure 19** shows the heat flow and time for the cooling of 8OCB LC with peaks for crystalline (k), smectic (sm) and nematic (n). **Figure 20** compares the temperature and heat flow of the phase peak whose data can be found in Table 2. **Figures 21-23** are comparisons of the heat flow and time using the quantitative representations of thermal speed, acceleration, and jerk, equations 11-13 were used to create the derived graphical representations using LoggerPro. The peak values for the derivative graphs are reported in Table 4. A similar relationship seen in segment 6, when compared to 2 can be seen in segment 8 when compared to 4. Though the temperature at which the phase changes occurred were relatively similar, the change in heat flow and movement of the particles has been greatly exaggerated with the increased flow rate of 10.0(K/min).

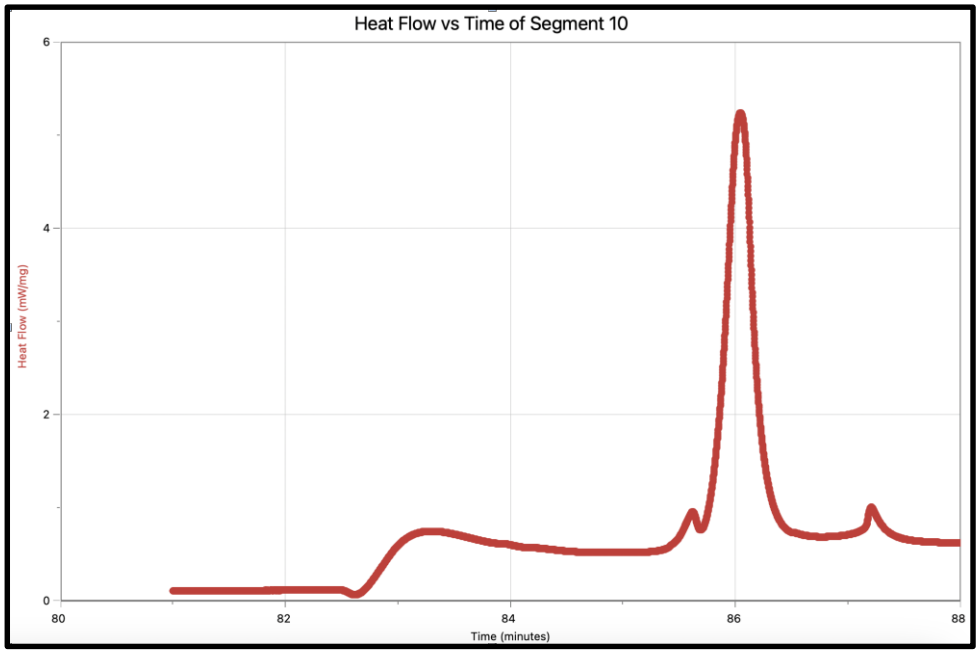

Figure 24. Heat flow vs. Temperature graph for 8OCB for heating at rate 20°C/min.

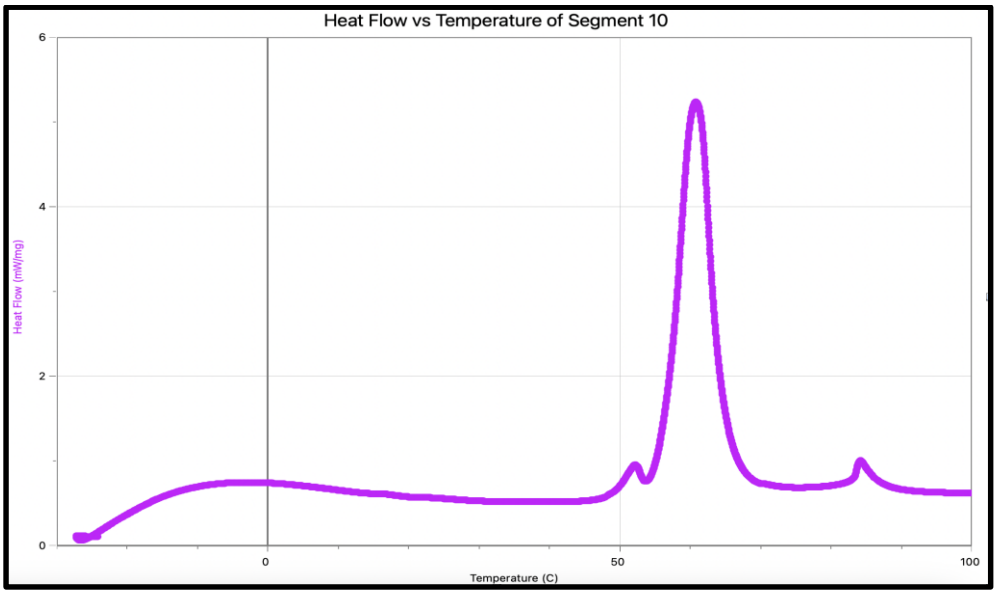

Figure 25. Heat flow vs. Time graph for 8OCB for heating at rate 20°C/min.

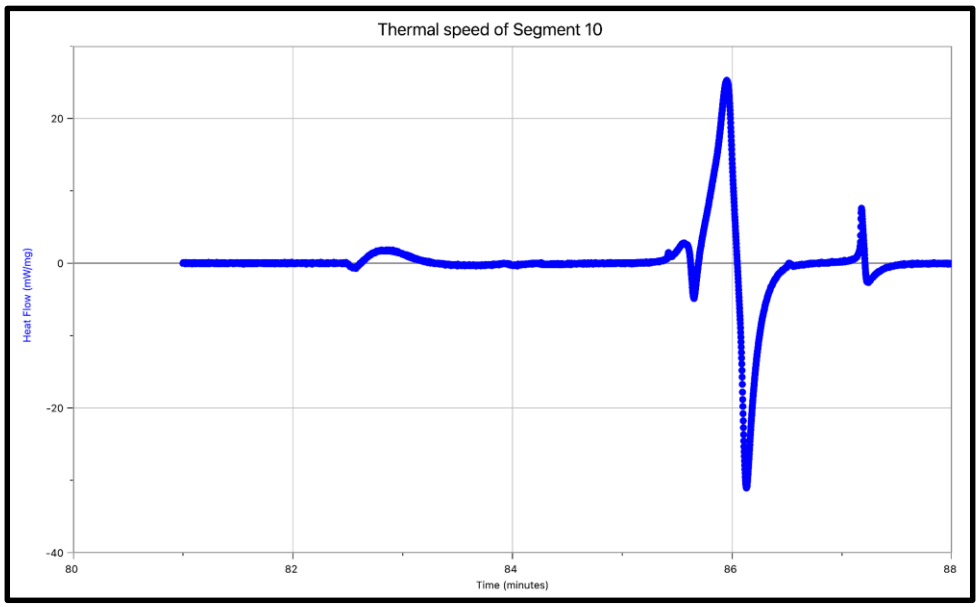

Figure 26. Thermal speed vs time graph for 8OCB for heating at rate 20°C/min.

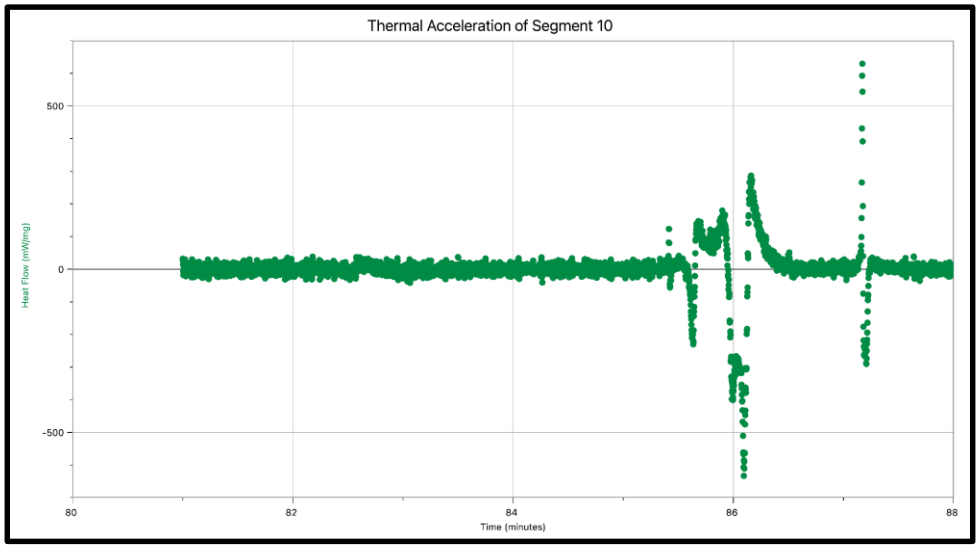

Figure 27. Thermal acceleration vs. Time graph for 8OCB for heating at rate 20°C/min.

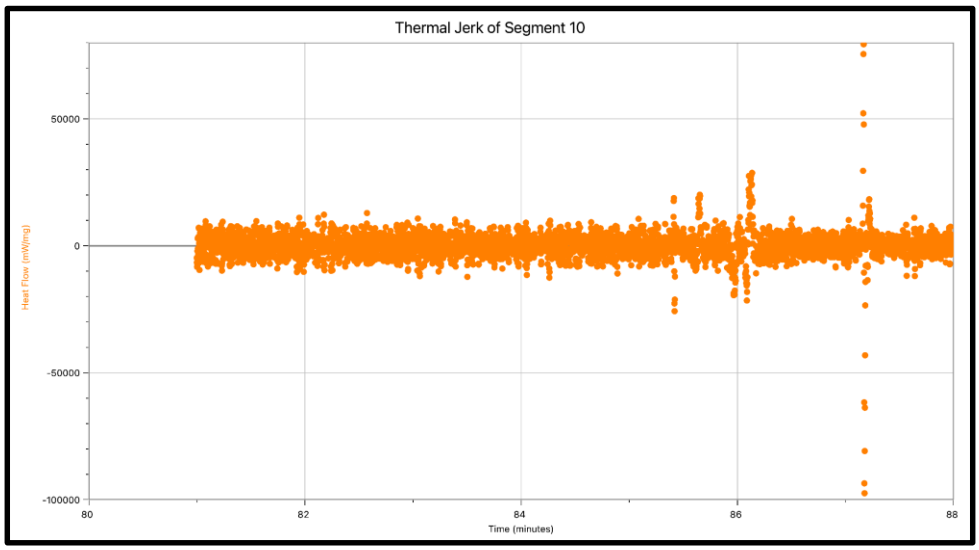

Figure 28. Thermal Jerk vs. Time graph for 8OCB for heating at rate 20°C/min.

Figures 24-28 represent the data collected for segment 2 (0°C/20.0(K/min)/100°C). **Figure 24** shows the heat flow and time for the heating of 8OCB LC with peaks for crystalline (k), smectic (sm) and nematic (n). **Figure 25** compares the temperature and heat flow of the phase peak whose data can be found in Table 2. **Figures 26-28** are comparisons of the heat flow and time using the quantitative representations of thermal speed, acceleration, and jerk, equations 11-13 were used to create the derived graphical representations using LoggerPro. The peak value for the derivative graphs are reported in Table 5. The phenomenon in segment 6 also occurs in segment 10 as **Figure 25** demonstrates the effects of increased heat flow rates as there is the absorbance of the smectic peak into the crystalline transition peak, supporting the increased heatflow times seen in Table 5 with less than 1.5 minutes between k_1 amd n_2

.

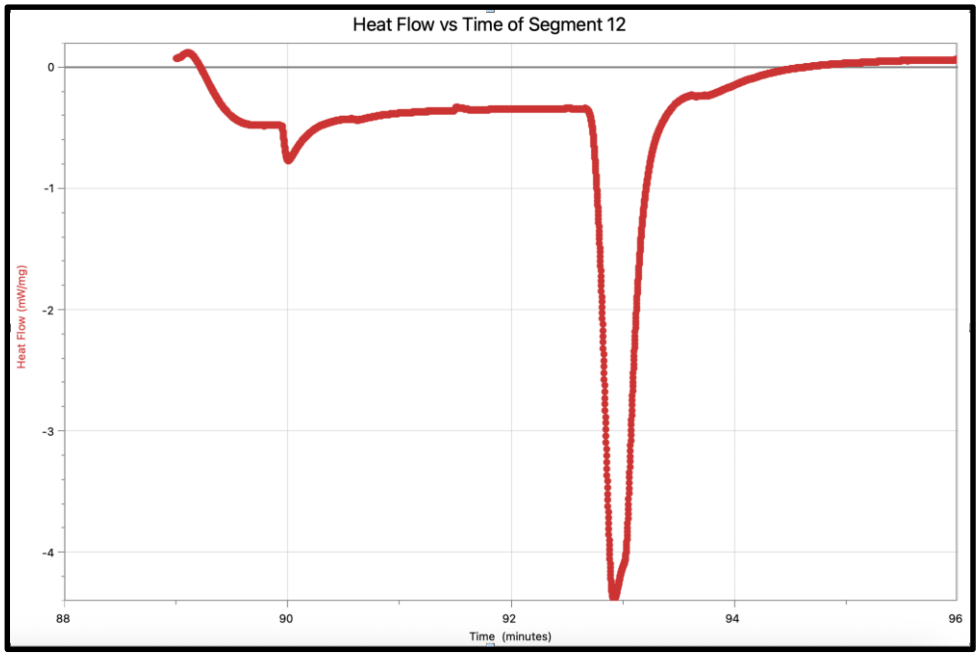

Figure 29. Heat flow vs. Time graph for 8OCB for cooling at rate 20°C/min.

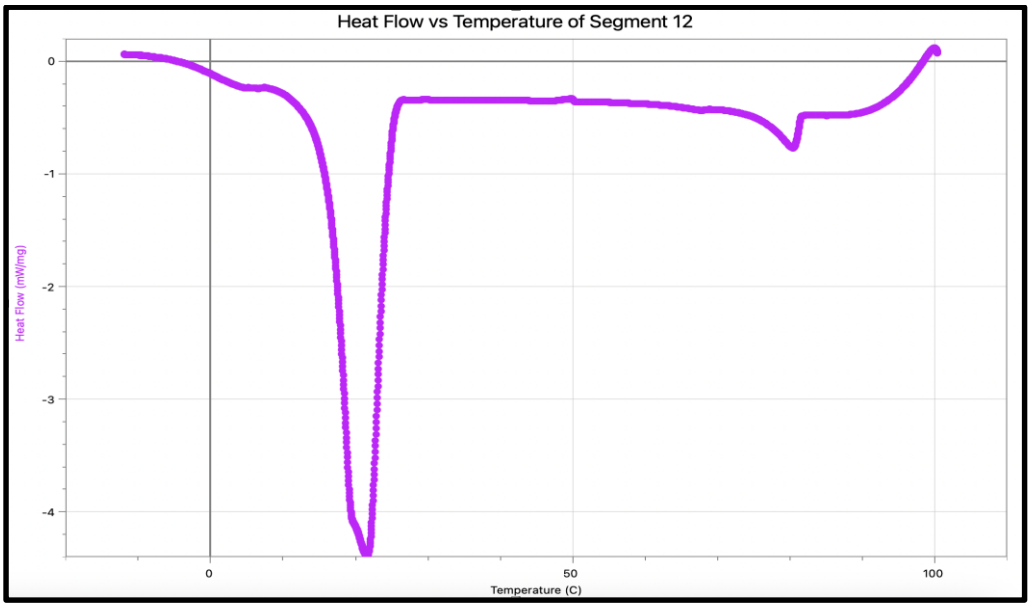

Figure 30. Heat flow vs. Temperature graph for 8OCB for cooling at rate 20°C/min.

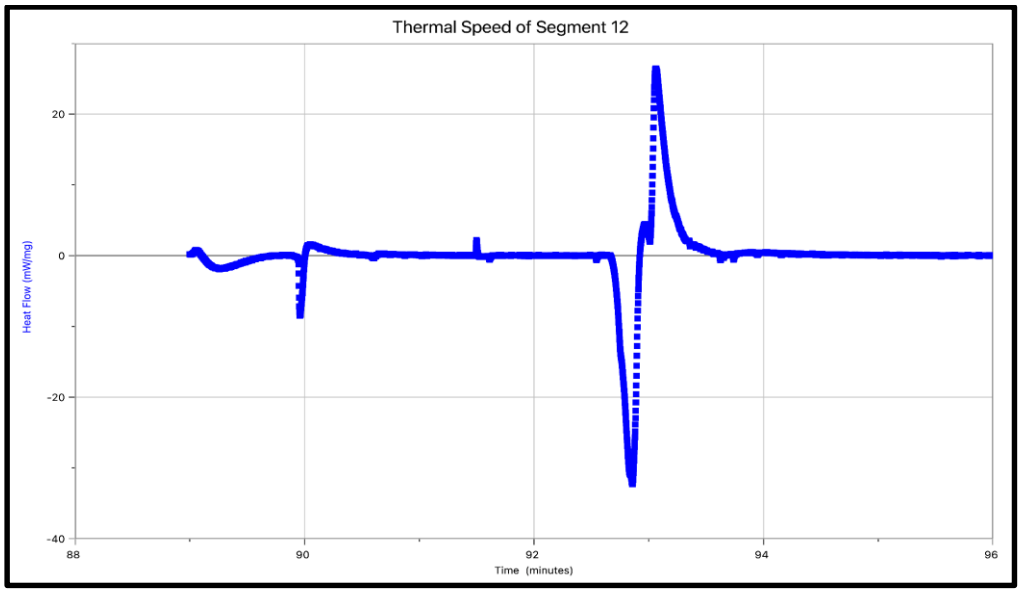

Figure 31. Thermal speed vs time graph for 8OCB for cooling at rate 20°C/min.

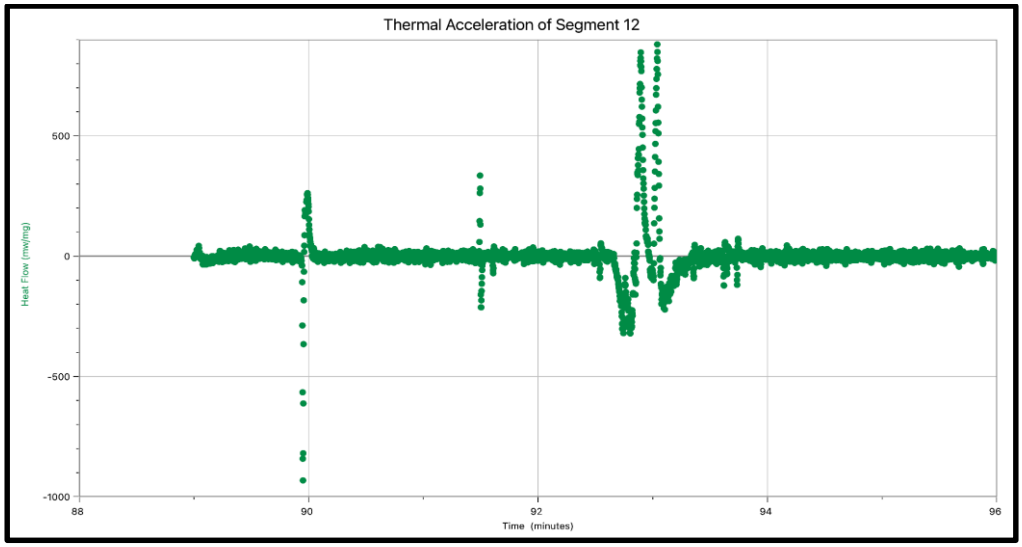

Figure 32. Thermal acceleration vs. Time graph for 8OCB for cooling at rate 20°C/min.

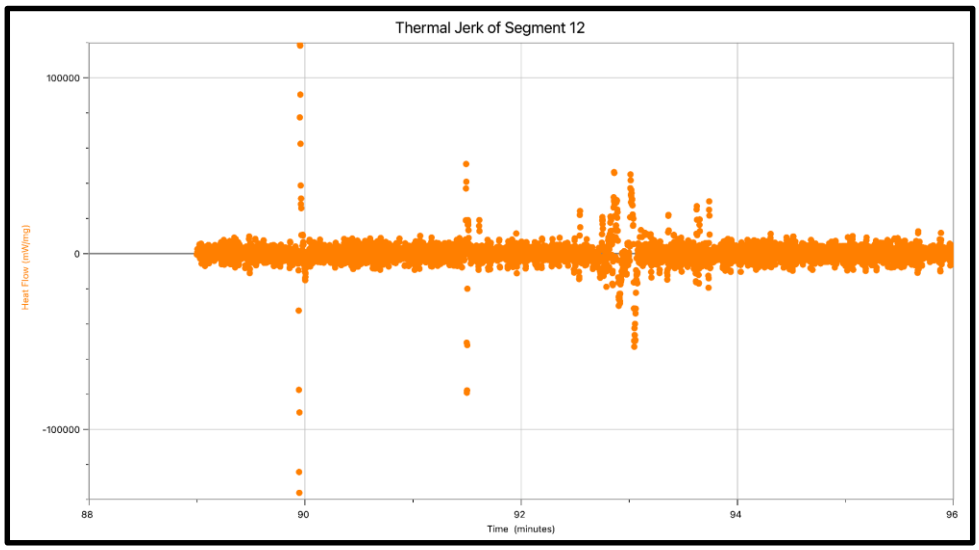

Figure 33. Thermal Jerk vs. Time graph for 8OCB for cooling at rate 20°C/min.

Figures 29-33 represent the data collected for segment 2 (0°C/20.0(K/min)/100°C). **Figure 29** shows the heat flow and time for the cooling of 8OCB LC with peaks for crystalline (k), smectic (sm) and nematic (n). **Figure 30** compares the temperature and heat flow of the phase peak whose data can be found in Table 2. **Figures 31-33** are comparisons of the heat flow and time using the quantitative representations of thermal speed, acceleration, and jerk, equations 11-13 were used to create the derived graphical representations using LoggerPro. The peak value for the derivative graphs are reported in Table 5. The overall thermal speed, acceleration and jerk followed the trend of increasing in intensity and down in less time than the heat flow rates of 5.0(K/min) and 10.0(K/min). It is important to note that the cooling derivatives did increase in speed, but, on average, were longer periods of time than the counterpart heating derivatives.

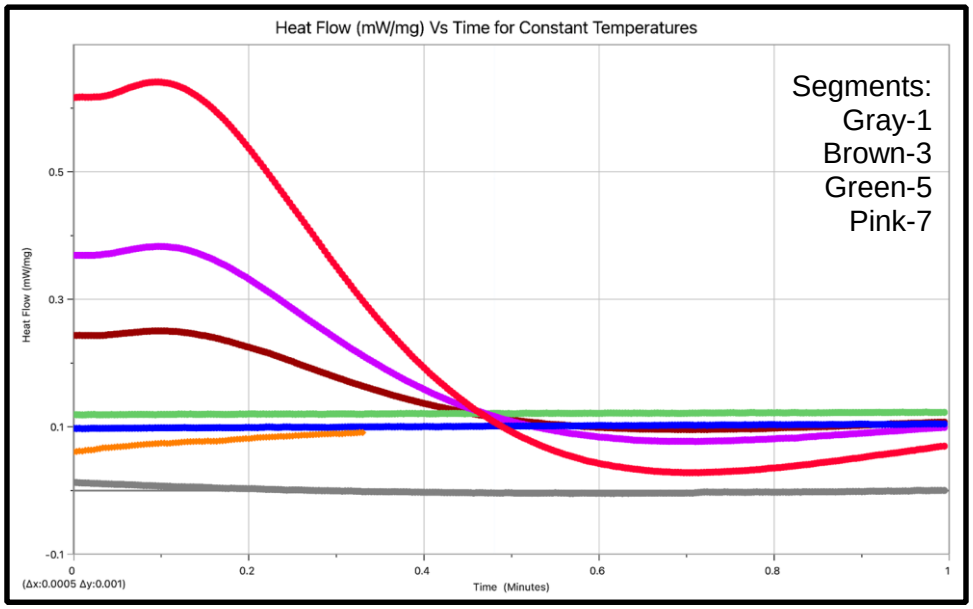

Figure 34. Heat flow vs. Time for segments 1, 3, 5, 7, 9, 11, 13.

Figure 34 showcases the heat flow of heat flow rates 5.0, 10 and 20(K/min). Segment 1 and 3 correspond to the rate of 5.0(K/min), segment 1 benign just before the ramp rate was introduced and segment 3 being just after the ramp rate was paused before 8OCB was cooled. Segment 5 is the transition between the heating of segment 6 at ramp rate of 10.0(K/min). This pattern continues with segment 7 preceding the cooling of segment 8, segment 9 preceding the heating of segment 10 at ramp rate 20.0(K/min), segment 11 preceding the cooling of segment 12 and segment 13 proceeding the cooling of segment 12. Comparing the iso-thermal phases 8OCB, there is a noticeable increase in heat flow in segments 1, 5 and 9, the phases before the segments were heated. There is also a noticeable increase steeped in the decrease of heat flow in segment 3, 7 and 11, relating to just before the segment was cooled. There is also a noticeable

increase of heat flow at the very beginning and tail end of the segments 3, 7 and 11.

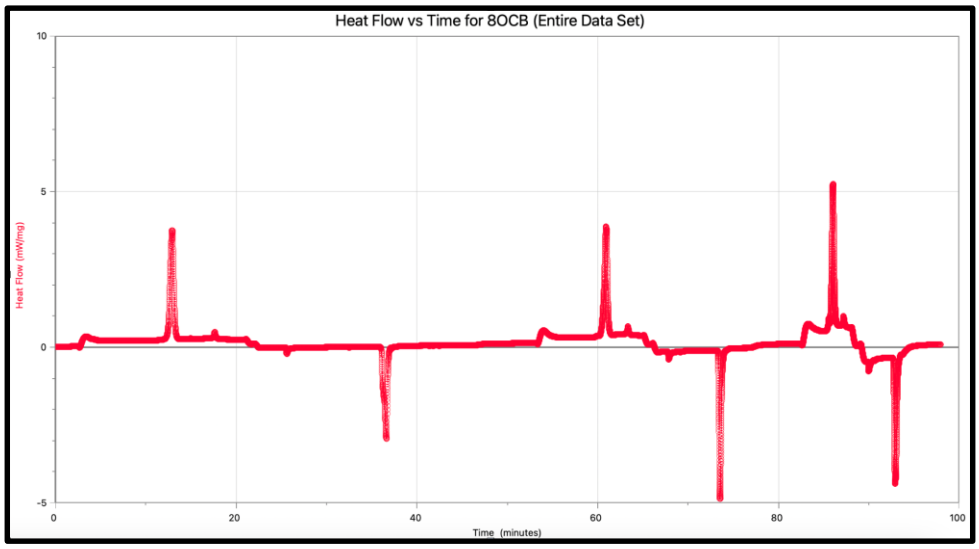

Figure 35. Heat flow vs. Time of entire data set for all three runs (5°C/min, 10°C/min and 20°C/min).

Figure 35 is a representation of the time and heat flow of 8OCB across the entire run of the DSC through the three ramp rates of 5.0, 10.0 and 20.0(K/min). There is the noticeable shortened frame of when the peaks occur, corresponding to the increased ramp rates as well as some increased speaking in the phase transition peaks. The individual segments can be seen broken down in **Figures 4, 9, 14, 19, 24 and 29**. The temperatures of the peaks shown above can be seen in Table 2. What can also be illustrated in this graph, can can bee seen in more detail in **Figures 8 and 4**, is just before the start of ramp rate 10.0 and 20.0(K/min), there is a slight step just before the isothermal segments (~45 and 75 minutes of the run).

DISCUSSION

This study aims to observe the liquid crystal properties of 4-oxy-4'-cyano-biphenyls, 8OCB by analyzing its behavior through the use of DSC and understanding how this thermotropic nature is affected by different rates of increasing and decreasing temperatures. The data collected from the DSC was analyzed using LoggerPro and graphically interpreting heat flow, temperature and time as it relates to the 3 main phase changes of 8OCB: crystalline to smectic and smectic to nematic. The stability of these phase changes are relevant to the context of LCDs as these displays rely heavily on the nematic and smectic phase transitions to be able to handle a variety of temperature ranges when continued amounts of electric currents are introduced to the LCs when a device is running.

Observing the preliminary analysis of 8OCB, found in Table 2, there appears to be consistent peaking of the crystalline, smectic and nematic peaks for the varying ramp rates of 5, 10, and 20 °C/min. The temperature differences were calculated into Tables 6 and 7 below for the heating and cooling of 8OCB across the DSC run:

Table 6. Temperature ranges for heating of 8OCB Liquid Crystal at varying ramp rates.

This table showcases the temperature changes of 8OCB from crystalline form to smectite (Rsm) and smectic to nematic (Rn) over the course of three different ramp rates, 5, 10, and 20 °C/min.

Rate °C/min	Cycle	Rsm (°C) k-sm	Rn(°C) of peak sm-n
5	Heat (seg. 2)	10.72	12.7
10	Heat (seg. 6)	10.64	13.26
20	Heat (seg. 10)	9.96	13.41

Table 7. Temperature ranges for cooling of 8OCB Liquid Crystal at varying ramp rates.
Below are the temperature ranges collected from nematic to smectite (Rn) and smectic back to crystalline (Rsm) for the ramp rates of 5, 10, and 20 °C/min.

Rate °C/min	Cycle	Rsm(°C) sm-k	Rn(°C) n-sm
5	Cool (seg. 4)	20.23	34.77
10	Cool (seg. 8)	22.99	34.39
20	Cool (seg. 12)	28.17	31.12

In regards to heating, there is very little variation found in Table 6 for the heating at three different ramp rates as the variations themselves for crystalline to smectic differentiate by 0.76 °C and 0.71 °C for the phase transition of smectic to nematic. This is not a traditional occurrence for the LC family of nCB, but the presence of oxygen greatly seems to affect the stability of the LC molecule. When compared to other members of the nOCB family, 6OCB also processes the property of sustaining similar phase change temperatures regardless of the ramp rate, however, 6OCB had lower temperatures overall for which the phase change occurred during the DSC [18]. 8OCB has the presence of oxygen, increasing the dipole moment, stabilizing the molecule during high temperatures and drastic heat flow changes relative to 6OCB and gas the addition of an 8OCB tail rather than 6OCB, increasing the weight and strength of the molecule over all [17]. These characteristics would also compare with 8OCB's counterpart 8CB of the nCB family as the addition of oxygen is both an increase in weight polarity due to the presence of oxygen. The stability of 8OCB at higher temperatures is further emphasized in the data found in Tables 3-5. With the increasing ramp rate, the transition from crystalline to smectic and smectic to nematic, though increase in temperature can still be seen as a distinct phase transition in **Figures 5, 15, and 25**. Though there is presumably a limit to the ramp rates and would have to be further studies to explore the limit to 8OCB and at what rate does its phase transitions become indistinguishable.

When looking at the motion of the molecules in non-isothermal moments, thermal speed acceleration and jerk are important indications to the amount of heat flow change the molecule can handle. When comparing phase transitions at ramp rate of 5°C/min and 20 °C/min, nematic was able handled heat flow speeds of 4,748 to -7923 and 78,833 - 97,162 ((mW/mg)/min) during heating. Tables 3-5 corroborate the intense acceleration and jerk 8OCB is able to handle during the heating and cooling process, but heating will mainly be focused on for this study. It is important to note that LCDs utilize both nematic and smectic displays . In this study smectic was seen to be able to handle intense changes in heat flow during the heating process, but when the ramp rate increased 10 and 15 °C/min, acceleration, and jerk were not always visible as the phase was being absorbed in the crystalline phase transition, seen in especially in 20 °C/min, **Figure 25** and Table 5. This would be important to keep in mind when designing LCDs that rely on smectic rather than nematic phase transitions for the desired polarizations in the displays as nematic appears to be more stable and consistent at higher temperatures and higher heating rates. This can further be corroborated by research performed on the LC 5OCB [21].

In regards to the isothermal behavior of 8OCB, found in **Figure 34**, an overall increase in heat flow can been seen in 8OCB as the ramp rates increase from 5 to 20 °C/min. For 5 °C/min, the starting heat flow before heating is around 0.0 mW/mg when the sample was held at 0 °C and then jumps to a maximum flow of 0.245 mW/mg when held at 100 °C and settles back down 0.1 mW/mg before cooled for segment 4. At 10 °C/min, the starting heat flow before heating rises to 0.12 mW/mg at 0 °C and then after heating of segment 6, rises to 0.369 mW/mg when held at 100 °C. This increase in heat flow in segment 1 compared to 5 can be accounted for by the step formation examined in **Figure 35** that occurs before the start of a new run, indicating that the liquid crystals are not completely returning to their original and complete crystalline state and retaining some of the heat previously acquired, starting the heating process off at high temperatures than initially. For 20°C/min, segment 13 has the most drastic increase in heat flow change going from a maximum of 0.64 mW/mg and settling to 0.07mW/mg.

These drastic heat flow changes over 1 minute for increasing temperature ramp rates speak to 8OCB's stability as before each heating and cooling. For before heating 8OCB relatively returns to a similar heat flow of around 0.1 mW/mg, increasing slightly form the initial almost 0.0 mW/mg, most likely due to retained heat causing steps in the runs discussed previously, but after the cooling of the 5, 10 and 20 °C/min,

the heat flow ranged from 0.092-0.122 mW/mg, speaking to 8OCB being able to return to a reliably organized state before being heated at different ramp rates. Even after 8OCB is heated, while the temperature is held at 100 °C, the heat flow is able to stabilize at 0.07-0.107 mW/mg, meaning it is ale to adjust and maintain a consistent heat flow during high temperatures of different ramp rates. 8OCB's isothermal nature, overall speaking highly to its stability as, even when temperature is constant, 8OCB is able to remain stable by adjusting its heat flow to relatively consistent value which is important when considering its durability and functionality in LCDs.

CONCLUSION

In this study the isothermal and non-isothermal behavior of LC 8OCB was explored to determine how it would react to increasing and decreasing temperatures at different rates of change. The relevance of this analysis relates to 8OCB's use in LCDs and how its immense stability would be helpful in technology that exists in hot environments. Regardless of the ramp rate for the heat introduction, 8OCB is stabilized enough, due to the added weight and dipole moment, to have consistent temperatures where phase changes for 8OCB occur. This would be most relevant for the heating of 8OCB as that is when the technology would be powered on, converting electrical to thermal energy to activate the polarization elements of the screen that occur during either smectic or nematic phases. 8OCB could heat up in environments with increasing high temperatures and maintain its phase change and have the ability to stabilize the heat flow even when the temperature is not moving. Also, when the technology cools down from not being used, 8OCB is able to return to similar phase transition conditions, allowing the LCD to start at about the same phase and LC arrangement which is important for functionality and consistency in technology performance. As the phases are also able to stabilize in isothermal conditions, this allows slower degradation of the LC and therefore LCD as 8OCB can maintain its distinct phase changes and their arrangement properties regardless of higher temperatures or increased ramp rates, especially when compared to 6OCB and 8OCB. Overall 8OCB would work well for LCDs in environments of higher temperatures due to the increased stability and consistency in phase transitions, especially regarding nematic LCDs.

REFERENCES

1. *Phases of matter*. (n.d.). Retrieved April 9, 2024, from https://www.grc.nasa.gov/www/k-12/airplane/state.html
2. *States of matter*. States of Matter | Chemical Instrumentation Facility | Iowa State University. (n.d.). https://www.cif.iastate.edu/services/acide/xrd-tutorial/matter
3. *What is an atom ?* (n.d.). NRC Web. Retrieved April 13, 2024, from https://www.nrc.gov/reading-rm/basic-ref/students/science-101/what-is-an-atom.html
4. *Brg—Introduction to liquid crystals*. (n.d.). Retrieved April 9, 2024, from https://barrett-group.mcgill.ca/tutorials/liquid_crystal/LC02.htm
5. Jain, A. K., & Deshmukh, R. R. (2020). An overview of polymer-dispersed liquid crystals composite films and their applications. In *Liquid Crystals and Display Technology*. IntechOpen. https://doi.org/10.5772/intechopen.91889
6. Axenov, K. V., & Laschat, S. (2011). Thermotropic Ionic Liquid Crystals. *Materials (Basel, Switzerland)*, *4*(1), 206–259. https://doi.org/10.3390/ma4010206
7. Differential scanning calorimetry. (2024). In *Wikipedia*. https://en.wikipedia.org/w/index.php?title=Differential_scanning_calorimetry&oldid=1209327516
8. Gill, P., Moghadam, T. T., & Ranjbar, B. (2010). Differential scanning calorimetry techniques: applications in biology and nanoscience. *Journal of biomolecular techniques : JBT*, *21*(4), 167–193.
9. Lcd history—Displaybly. (n.d.). Https://Displaybly.Com/. Retrieved April 9, 2024, from https://displaybly.com/lcd-history/
10. Liquid crystals. (n.d.). Retrieved April 9, 2024, from https://www.ch.ic.ac.uk/local/projects/abbott/LCDs.htm
11. *Liquid crystal displays*. (n.d.). Retrieved April 13, 2024, from https://web.media.mit.edu/~stefan/liquid-crystals/node3.html
12. Observance of multiple melting and nematic phase transitions in a next generation quaternary liquid crystal system(Qlcs). (n.d.). Retrieved April 9, 2024, from https://www.pubtexto.com/pdf/?observance-of-multiple-melting-and-nematic-phase-transitions-in-a-next-generation-quaternary-liquid-crystal-system-qlcs
13. Liquid crystal display (Lcd) | Britannica. (n.d.). Retrieved April 9, 2024, from https://www.britannica.com/technology/liquid-crystal-display
14. admin. (2021, May 17). Nematic vs smectic phase in lcds. Nelson Miller. https://nelson-miller.com/nematic-vs-smectic-phase-in-lcds/
15. Ghosh, S., & Roy, A. (2021). Crystal polymorphism of 8OCB liquid crystal consisting of strongly polar rod-like molecules. *RSC Advances*, *11*(9), 4958–4965. https://doi.org/10.1039/D0RA08543J

16. Selevou, A., Papamokos, G., Steinhart, M., & Floudas, G. (2017). 8ocb and 8cb liquid crystals confined in nanoporous alumina: Effect of confinement on the structure and dynamics. *The Journal of Physical Chemistry B*, *121*(30), 7382–7394. https://doi.org/10.1021/acs.jpcb.7b05042
17. Seide, M., Doran, M. C., & Sharma, D. (2022). Analyzing nematic to isotropic (N-i) phase transition of ncb liquid crystals using logger pro. *European Journal of Applied Sciences*, *10*(3), 98–124. https://doi.org/10.14738/aivp.103.12373
18. Mello, J. (2022). Details of Nematic Phase Transition and Nematic Range of 5OCB Liquid Crystal using Logger Pro. *International Journal of Research in Engineering and Science*, *10*(9), 197–217. https://www.ijres.org/papers/Volume-10/Issue-9/1009197217.pdf
19. Vernier. (2019). Logger Pro® 3 - Vernier. Vernier. https://www.vernier.com/product/logger-pro-3/
20. admin. (2021, May 17). Nematic vs smectic phase in lcds. *Nelson Miller*. https://nelson-miller.com/nematic-vs-smectic-phase-in-lcds/
21. Mello, J., & Sharma , D. (2022). Effect of Reheating and Ramp Rates on Phase Transitions of 5OCB Liquid Crystal using Logger Pro. *International Journal of Research in Engineering and Science (IJRES)*, *10*(9), 218–236. https://www.ijres.org/papers/Volume-10/Issue-9/1009218236.pdf